JACS
JOURNAL OF THE AMERICAN CHEMICAL SOCIETY
Communication
pubs.acs.org/JACS

Mechanistic Explanation of the pH Dependence and Onset Potentials for Hydrocarbon Products from Electrochemical Reduction of CO on Cu (111)

Hai Xiao, Tao Cheng, William A. Goddard III,* and Ravishankar Sundararaman

Materials and Process Simulation Center (MSC) and Joint Center for Artificial Photosynthesis (JCAP), California Institute of Technology, Pasadena, California 91125, United States

Supporting Information

ABSTRACT: Energy and environmental concerns demand development of more efficient and selective electrodes for electrochemical reduction of CO_2 to form fuels and chemicals. Since Cu is the only pure metal exhibiting reduction to form hydrocarbon chemicals, we focus here on the Cu (111) electrode. We present a methodology for density functional theory calculations to obtain accurate onset electrochemical potentials with explicit constant electrochemical potential and pH effects using implicit solvation. We predict the atomistic mechanisms underlying electrochemical reduction of CO, finding that (1) at acidic pH, the C_1 pathway proceeds through COH to CHOH to form CH_4 while C_2 (C_3) pathways are kinetically blocked; (2) at neutral pH, the C_1 and C_2 (C_3) pathways share the COH common intermediate, where the branch to C−C coupling is realized by a novel CO−COH pathway; and (3) at high pH, early C−C coupling through adsorbed CO dimerization dominates, suppressing the C_1 pathways by kinetics, thereby boosting selectivity for multi-carbon products.

Electrochemical reduction of CO_2 (CO2RR) to fuel and chemical products using renewable electricity is a promising technique to achieve carbon neutrality under mild conditions. Copper is the only known electrode material that delivers appreciable amounts of hydrocarbons, primarily methane and ethylene, with minor alcohol products.[1−6] However, Cu exhibits high overpotentials and a lack of selectivity that precludes economic applications. For practical electrochemical reduction of CO_2 to fuels and chemicals, it is essential to find a new more efficient and more selective electrode.

To provide guidelines for such rational design, we apply quantum mechanics (QM) methods to develop a mechanistic understanding of the processes on Cu. We want to emphasize at the beginning that there are many uncertainties on how to use QM to obtain reliable predictions about electrocatalysis. To be useful in guiding design and comparing to experiment, it is essential that the reaction barriers be accurate to ∼0.1 eV and that the predicted onset potentials be accurate to ∼0.1 V. To be practical, we need to use density function theory (DFT), but major questions arise as to which "flavor" to use: LDA, PBE, B3LYP, M06, etc. Moreover, to be practical, the number of atoms per unit cell must be limited to ∼200 atoms, which creates severe limitations on how the solvent is treated. Do we use a continuum solvent description, and which one, or do we try to include part of the solvent explicitly? The experiments are done under conditions in which the applied potiential is fixed, whereas calculations are far easier to apply to the condition of constant number of electrons. How do we use the QM to relate to the experimental conditions? The experiments are referenced to the standard hydrogen electrode (SHE) at which the free energy of a proton at pH = 0 is in equilibrium with H_2 gas at standard conditions, whereas the theory most conveniently deals with the Fermi energy with respect to the vacuum. How should we handle this? The relevant quantities in rates are free energies at the reaction temperature, whereas the QM most easily deals with the energies or enthalpies. For each of these issues, it is difficult to validate against experiment because discrepancies might involve various combinations of all the approximations. Instead our strategy is to tackle all the above issues simultaneously with methods that we consider likely to be both valid and practical, and we test all the approximations simultaneously by predicting how the results depend on experimental variables such as pH and applied potiential for a system where the experiments have been done very carefully and where it is known that the product ratios and rates depend sensitively on the pH and potential. Indeed, for CO2RR on Cu (111), we find excellent agreement with experiment for the onset potentials of producing various hydrocarbon products over the range of pH from 1 to 13.

We claim that this excellent agreement with experiment for the calculations reported here validates that the particular combination of choices we have made is sufficiently accurate for the particular problem we have chosen to address, providing a sound basis on which to tackle other electrochemical catalysis problems. This provides a starting point for studies of other electrochemical systems, such as CO2RR on other surfaces of Cu, on alloys of Cu, and on other metals, metal oxides, metal nitrides, etc. Moreover, it provides a starting point to consider other electrochemical processes such as ORR, OER, etc. Our plan is to procced cautiously with other sytems using the same combinations of methods to predict the properties of new electrocatalysts for systems that can be studied experimentally. We expect that this will lead gradually to developing a validated QM-based technology for making reliable predictions on

Received: October 30, 2015
Published: December 30, 2015

DOI: 10.1021/jacs.5b11390
J. Am. Chem. Soc. 2016, 138, 483−486

electrocatalysis in advance of experiment. This paper is meant to provide the first step toward this goal. In addition, it provides a detailed reaction mechanism explaining the very complex ways that the products of CO2RR on Cu (111) depend on applied potential and pH, which we expect to be useful in designing modified catalysts or conditions.

In CO_2 reduction on Cu, CO is produced at the lowest overpotential and the electrochemical reduction of CO gives the same product spectrum as that of CO_2.[7,8] Thus, it is believed that CO is the essential intermediate linking CO_2 to more reduced products, and we focus here electrochemical reduction of CO.

Several QM computational investigations have suggested rationalizations of experimental results[3−5,8−10] in terms of postulated mechanisms for CO electrochemical reduction (COER) on Cu surfaces. In 2010, Peterson et al.[11] examined this reaction for the Cu (211) surface and suggested a pathway along which the potential-limiting step is formation of CHO_{ad} from protonation of CO_{ad}, concluding that CHO_{ad} leads to both CH_4 and C_2H_4. These calculations did not calculate reaction barriers and ignored solvation. Similar studies were reported by Calle-Vallejo et al.,[12] who proposed instead that C_2 products arise from C−C coupling between two CO_{ad}. These studies ignored reaction barriers and solvation and did not predict overpotentials and selectivity.

In 2013, Nie et al.[13] reported transition states (TSs) for COER on Cu (111) but without full solvation. They concluded that the COH_{ad} is the kinetically dominant key intermediate, leading to CH_x (x = 0−4) species sequentially. C_2H_4 was proposed to form at the CH_2 step, although this contradicts the experimental conclusion that pathways to CH_4 and C_2H_4 branch at an early stage of COER.[9,14] Indeed, Montoya et al.[15] calculated the barriers of CO dimerization on Cu (111) and (100) and found them to be sufficiently low for C−C coupling to proceed early. This study used only a simple charged water layer to mimic the electrochemical environment for highly negative applied potentials.

In addition to ignoring full effects of solvent, all previous theoretical studies assumed constant numbers of electrons (N_e), whereas experimental electrochemical half-cells are open systems operating at constant electrochemical potentials (μ_e). The calculations with constant N_e suffer from large variations in μ_e, leading to increases of ∼1 V in modeling CO dimerization.[15] (The $\mu_e N_e$ contribution to free energies introduces significant deviations in the calculated reaction energy landscapes from the true values of constant μ_e systems.) Such inconsistencies preclude quantitative estimates of onset potentials.

Moreover, previous studies examined *only* C_1 or C_2 pathways, whereas the major selectivity issue in COER is the competition *between* C_1 and C_2 pathways. Here pH is an ineluctable factor to consider, as shown by recent experiments.[16] Indeed, we show here that this selectivity is strongly influenced by pH, making it essential to include pH effect in determining selectivity.

First we establish a DFT methodology to predict onset potentials, which we combine with pH effects and implicit solvation to explicitly calculate the reactions at constant μ_e. This allows us to elucidate the competition among possible pathways of COER on Cu at various pH, by calculating the free energy profiles while including both potential and pH dependence. Thus, we predict the onset potentials for CH_4 and C_2H_4 as a function of pH, leading to excellent agreement with experiment. We also find a C_3 pathway, observed experimentally to account for a few percent products. Thus, we consider that the results in this paper validate the particular combinations of methods we have chosen. In addition, the mechanism established in this study provides insights likely to be essential for designing new electrodes to achieve high selectivity with low overpotentials.

In modeling the electrochemical half-cell, we assume that this open system is at dynamic equilibrium with a constant applied potential U, while the proton source (H_3O^+ or H_2O) and electron source are refilled instantly prior to every electrochemical reaction step. Thus, we can approximate the half-cell with a closed system in which the reaction energy profile is obtained using standard DFT techniques [see Supporting Information (SI) for details]. For a protonation step, our model uses a hydrogen atom bonded to the surface to locate the TS and then references this back to the $H^+(H_3O^+/H_2O) + e^-$ pair through H_2 (details in SI). Thus, our model restores the reference energy of the correct initial state for the reaction energy profile, allowing the pH dependence to be introduced naturally.

Furthermore, we perform explicit constant μ_e calculations for all states along the reaction coordinate. This is done through variationally optimizing N_e to minimize the grand free energy at fixed μ_e, and the resulted net electronic charge is balanced by ionic screening in the electrolyte,[17] which is treated here using the CANDLE implicit solvation model.[18] Consequently this provides a realistic description of the electrochemical interface,[19] which includes both the external potential and solvation effects (details in SI). The final free energy profiles include zero-point energy, enthalpy, and entropy contributions from vibrations of surface species. For example, the free energy barrier $\Delta G^‡$ for COH formation is given by

$$\Delta G^‡(\mathrm{COH}) = 0.63 + 0.0592 \times \mathrm{pH} - 0.0959 \times U(\mathrm{eV})$$

while $\Delta G^‡$ for CO dimerization is given by

$$\Delta G^‡(\mathrm{CO{-}CO}) = 1.15 + 0.0510 \times U(\mathrm{eV})$$

where U is referenced to the SHE. Note that $\Delta G^‡(\mathrm{CO{-}CO})$ is independent of pH, since no proton is involved in the reaction.

The minimal onset potential for each step is simply

$$|U|_{\min} = \max(\Delta G^‡, \Delta G)/e$$

where $H^+(H_3O^+/H_2O) + e^-$ for each step provides the energy input of eU. Here we must compare both $\Delta G^‡$ and ΔG because for some ranges of U, the TS can be lower in energy than the final state for some reactions, making the step a simple uphill process.

We use the PBE flavor of DFT theory, as implemented in VASP using cutoffs and core effective potentials (pseudopotentials) as described in the SI.

The Cu (111) surface serves as a simple but useful model for validating our particular combination of methods since accurate experimental data are available showing a broad range of chemistries[20] with strong pH- and potential-dependent selectivity.[16] The pathways considered are shown in Figure 1:

- starting from adsorbed CO, the (R1) COH and (R2) CHO pathways for protonation and the (R3) CO−CO path for dimerization constitute all competing options;
- the COH path (R1) further branches into three channels: advancing along the C_1 path through either (R1a) the C path[13] by removing the OH group or (R1b) the CHOH path, and more interestingly, opening up a

DOI: 10.1021/jacs.5b11390
J. Am. Chem. Soc. 2016, 138, 483−486

new C_2 path by C−C coupling through (R1c) the CO−COH path;

- the CHO path (R2) converges with the COH path (R1b) at the point of forming CHOH while the CO−CO path (R3) converges with the CO−COH path (R1c) at the point of forming the COCOH adsorbate.

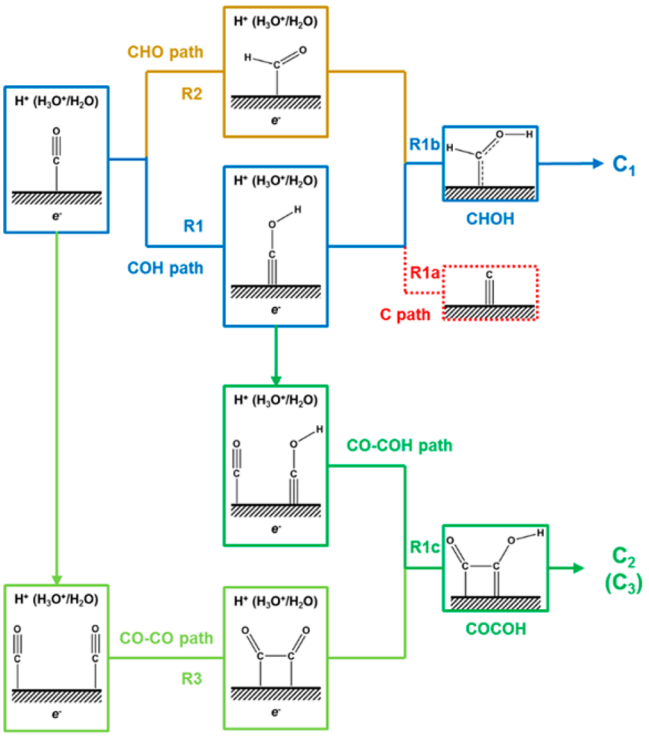

Figure 1. Pathways for the first two steps of COER.

All free energy profiles including the pH and U dependence are listed in the SI. This is the first proposal of C−C coupling through the CO−COH path. It leads to a much lower barrier of 0.87 eV at U = 0 V than the 1.15 eV barrier for the CO−CO path, (previously proposed as the path to C_2 products).[12,15] This low barrier arises from the ability of COH adsorbate to acquire radical character (see discussion in the SI), which remains in the COCOH adsorbate until it forks to a new C_3 path by further coupling with another CO (discussed in the SI). This might explain why up to 4% C_3 products are observed experimentally, but not beyond C_3.[5]

For C_1 pathways, all reactions are modeled at the low coverage limit (θ_{CO} = 1/9 or 1/16, see Table S1) assuming universal availability of surface hydrogen. Since C−C coupling must start with a local coverage of 4/9, we provide a penalty of 0.12 eV[21] for this C_2 pathway to put it on an equal footing with the C_1 pathway. This accounts for the energy cost of switching H with CO to achieve the high local θ_{CO}.

To determine the onset potentials, we consider three typical experimental situations, pH = 1, 7, or 12.

Case A: At pH = 1 (Figure 2), the earliest onset potential of −0.80 V starts the C_1 path through COH formation, while the CHO and CO−CO paths lead to barriers higher by 0.08 and 0.43 eV, corresponding to kinetic rate ratios at 300 K of 4×10^{-2}:1 and 5×10^{-8}:1 to the COH path, respectively. Although their barriers show a positive dependence on U, it requires potentials as negative as −1.75 for CHO and −3.95 V for CO−CO paths, to have kinetics comparable with the COH path.

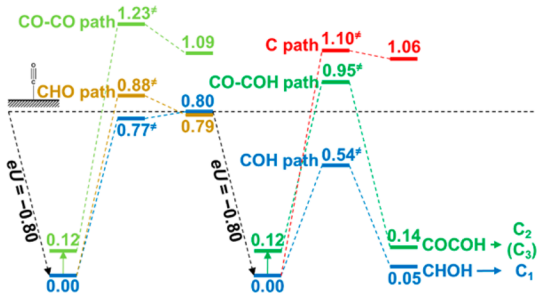

Figure 2. COER free energy profiles at pH = 1. The blue line shows the only pathway with significant rates. The predicted onset potential of −0.80 is in excellent agreement with the experimental value of −0.76 V (vs SHE) for CH_4.[16]

Following COH formation, the lowest barrier C_1 path proceeds through $CHOH_{ad}$ (instead of the previously proposed C_{ad},[13] which has a barrier 0.56 eV higher), while the new C_2 branch which proceeds by the CO−COH path, is suppressed by kinetics (a rate lower by 1×10^{-7}:1 at 300 K compared to the CHOH path). Thus, both C−C coupling mechanisms are blocked kinetically. Consequently there are essentially no C_2 products at pH = 1. This is consistent with the experimental observation that no C_2H_4 is produced on Cu (111) at pH = 1.[16] Our predicted onset potential of −0.80 V for C_1 products is in excellent agreement with the experimental value of −0.76 V (vs SHE) for CH_4.[16]

Case B: At pH = 7 (Figure 3), the COH path is again first with a predicted onset potential of −1.17 V. The CHO and CO−CO pathways are now accessible by kinetic rate ratios at 300 K of 0.1:1 and 0.2:1 to the COH path, respectively. More interestingly, along the dominant COH path, the branch into C_2 products through CO−COH coupling is also viable kinetically, with rate ratio at 300 K of 0.2:1 to the C_1 channel through the CHOH path. Consequently the C_1 and C_2 pathways share the COH_{ad} common intermediate. This confirms the experimental conclusion[10] on Cu (111) at pH = 7 that the pathway to C_2H_4 has a common intermediate with that to CH_4 (based on the same potential dependence, although the common intermediate was incorrectly speculated to be the CHO_{ad}). Our predicted onset potential of −1.17 V for the COH path agrees with the experimental value of −1.21 V for both CH_4 and C_2H_4,[10] and our predicted rate ratio of 0.2:1 for C_2:C_1 along the major COH path agrees with the experimental C_2H_4:CH_4 product ratio of 0.2:1.[20]

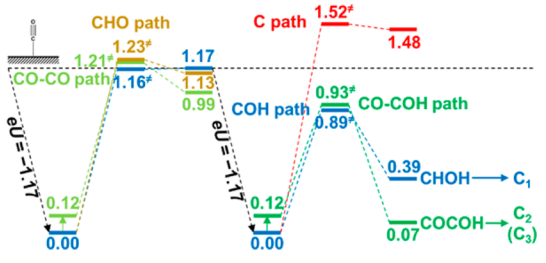

Figure 3. COER free energy profiles at pH = 7. The blue line indicates the dominant path, but we predict that the rate for the green line is 20% of that for the blue line, in agreement with the experimental C_2H_4:CH_4 product ratio of 0.2:1.[20] Our predicted onset potential of −1.17 V for the COH path agrees with the experimental value of −1.21 V for both CH_4 and C_2H_4.[10]

DOI: 10.1021/jacs.5b11390
J. Am. Chem. Soc. 2016, 138, 483−486

Case C: At pH = 12 (Figure 4), the CO−CO path is now initiated at the onset potential of −1.21 V, which agrees with the experimental value of −1.26 V for C_2H_4 production at pH = 12 on Cu (111).[16] Here, both C_1 pathways through COH_{ad} and CHO_{ad} are kinetically inhibited, by rate ratios at 300 K of $\sim 10^{-5}$:1 compared to the CO−CO path. Indeed the experiments report very small amounts of CH_4 with an onset potential of −1.46 V.[16] This might originate from isolated surface regions where sufficiently high local θ_{CO} for C−C coupling cannot be reached, due for example, to defects or inhomogeneities in the CO distribution, in which case C_1 pathways might be the only option (if so, our results predict onset potentials for COH and CHO paths of −1.48 and −1.51 V, respectively, in agreement with the experimental values). Nevertheless, the experiments suggested that local high pH might contribute to suppressing formation of CH_4.[14] High pH was used in the case where only C_2 and C_3 products are produced.[22] These results are consistent with our suggestion that high pH boosts selectivity for C_2 and C_3 products by kinetically blocking C_1 pathways. But a major possible complication is the promotion of the hydrogen evolution reaction (HER) by high pH, which reduces the Faraday efficiency of COER.

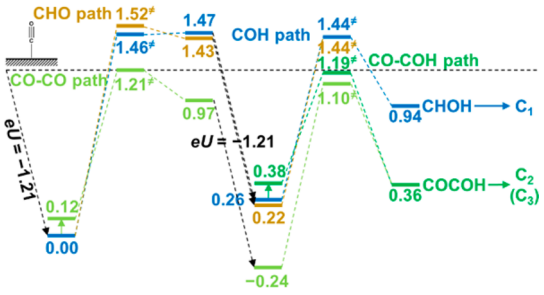

Figure 4. COER free energy profiles at pH = 12. The light green line shows the dominant pathway (by a factor of 10^5 at 300 K). The predicted onset potential of −1.21 V agrees with the experimental value of −1.26 V for C_2H_4 production at pH = 12.[16]

Summarizing, we demonstrate a new methodology for accurate prediction of onset potentials from QM calculations while including the pH-dependent mechanisms underlying selectivity for C_1 vs C_2 (C_3) products of COER on Cu (111). At low pH = 1, we find that multi-carbon production is suppressed kinetically, so that the C_1 pathway proceeds through COH_{ad} to $CHOH_{ad}$ formation. At neutral pH, we identify a common intermediate COH_{ad} for the major mechanism that branches into C_1 and C_2 (C_3) production. At high pH = 12, we find that selectivity for multi-carbon products arises by kinetically blocking C_1 pathways. Of course to selectively produce these C containing products, we must poison the HER, e.g., structurally engineering Cu to behave like the oxide-derived surface.[22] We consider that these excellent results with experiment validate the particular combination of methods used here, justifying this as the starting point for examinating other electrochemical reactions.

■ ASSOCIATED CONTENT

Supporting Information

The Supporting Information is available free of charge on the ACS Publications website at DOI: 10.1021/jacs.5b11390.

Figures S1−S4 and Tables S1−S4, computational details, free energy profiles, radical character of COH_{ad} branch to C_3 pathway, and coordinates for all structures (PDF)

■ AUTHOR INFORMATION

Corresponding Author

*wag@wag.caltech.edu

Notes

The authors declare no competing financial interest.

■ ACKNOWLEDGMENTS

This work was supported by the Joint Center for Artificial Photosynthesis, a DOE Energy Innovation Hub, supported through the Office of Science of the U.S. Department of Energy under Award No. DE-SC0004993. We are grateful to Dr. Robert J. Nielsen, Dr. Manny Soriaga, and Mr. Yufeng Huang for helpful discussions. The computations were carried out on computing resources Zwicky (Caltech) and NERSC.

■ REFERENCES

(1) Hori, Y.; Kikuchi, K.; Suzuki, S. *Chem. Lett.* **1985**, *14*, 1695.
(2) Hori, Y.; Wakebe, H.; Tsukamoto, T.; Koga, O. *Electrochim. Acta* **1994**, *39*, 1833.
(3) Hori, Y. In *Modern Aspects of Electrochemistry*; Vayenas, C., White, R., Gamboa-Aldeco, M., Eds.; Springer: New York, 2008; Vol. *42*, p 89.
(4) Gattrell, M.; Gupta, N.; Co, A. *J. Electroanal. Chem.* **2006**, *594*, 1.
(5) Kuhl, K. P.; Cave, E. R.; Abram, D. N.; Jaramillo, T. F. *Energy Environ. Sci.* **2012**, *5*, 7050.
(6) Kuhl, K. P.; Hatsukade, T.; Cave, E. R.; Abram, D. N.; Kibsgaard, J.; Jaramillo, T. F. *J. Am. Chem. Soc.* **2014**, *136*, 14107.
(7) Hori, Y.; Murata, A.; Takahashi, R.; Suzuki, S. *J. Am. Chem. Soc.* **1987**, *109*, 5022.
(8) Hori, Y.; Takahashi, R.; Yoshinami, Y.; Murata, A. *J. Phys. Chem. B* **1997**, *101*, 7075.
(9) Schouten, K. J. P.; Kwon, Y.; van der Ham, C. J. M.; Qin, Z.; Koper, M. T. M. *Chem. Sci.* **2011**, *2*, 1902.
(10) Schouten, K. J. P.; Qin, Z.; Gallent, E. P.; Koper, M. T. M. *J. Am. Chem. Soc.* **2012**, *134*, 9864.
(11) Peterson, A. A.; Abild-Pedersen, F.; Studt, F.; Rossmeisl, J.; Nørskov, J. K. *Energy Environ. Sci.* **2010**, *3*, 1311.
(12) Calle-Vallejo, F.; Koper, M. T. M. *Angew. Chem., Int. Ed.* **2013**, *52*, 7282.
(13) Nie, X.; Esopi, M. R.; Janik, M. J.; Asthagiri, A. *Angew. Chem., Int. Ed.* **2013**, *52*, 2459.
(14) Roberts, F. S.; Kuhl, K. P.; Nilsson, A. *Angew. Chem., Int. Ed.* **2015**, *54*, 5179.
(15) Montoya, J. H.; Shi, C.; Chan, K.; Nørskov, J. K. *J. Phys. Chem. Lett.* **2015**, *6*, 2032.
(16) Schouten, K. J. P.; Pérez Gallent, E.; Koper, M. T. M. *J. Electroanal. Chem.* **2014**, *716*, 53.
(17) Gunceler, D.; Letchworth-Weaver, K.; Sundararaman, R.; Schwarz, K. A.; Arias, T. A. *Modell. Simul. Mater. Sci. Eng.* **2013**, *21*, 074005.
(18) Sundararaman, R.; Goddard, W. A. *J. Chem. Phys.* **2015**, *142*, 064107.
(19) Schwarz, K. A.; Sundararaman, R.; Moffat, T. P.; Allison, T. C. *Phys. Chem. Chem. Phys.* **2015**, *17*, 20805.
(20) Hori, Y.; Takahashi, I.; Koga, O.; Hoshi, N. *J. Mol. Catal. A: Chem.* **2003**, *199*, 39.
(21) Zhang, Y.-J.; Sethuraman, V.; Michalsky, R.; Peterson, A. A. *ACS Catal.* **2014**, *4*, 3742.
(22) Li, C. W.; Ciston, J.; Kanan, M. W. *Nature* **2014**, *508*, 504.

DOI: 10.1021/jacs.5b11390
J. Am. Chem. Soc. 2016, 138, 483−486